Theor Chem Acc (2006) 116: 219–231
DOI 10.1007/s00214-005-0038-4

REGULAR ARTICLE

Ilaria Ciofini

Exploring the photophysical behaviour of supramolecular systems: problems and perspectives

Received: 2 April 2005 / Accepted: 4 October 2005 / Published online: 6 December 2005

Abstract The study of the photophysical properties of supramolecular systems, such as photochemical molecular devices (PMD), is intrinsically related to the possibility of correctly describing ground and excited state properties of large systems containing transition metal atoms.

Here we analyse the performance of density functional theory (DFT) and time dependent DFT in the evaluation of the photochemical behaviour of supramolecular systems aimed to produce photoinduced long-lived charge-separated states. Such PMDs are of great experimental interest as functional models for many chemical applications as, for instance, artificial photosynthesis. From a theoretical point of view, the challenge of these systems is not simply related to their size but also to the possibility of describing the " *emergence*" of new properties, involving the molecule as a global unit, using the tools provided by quantum chemistry.

Keywords Photochemical molecular devices (PMD) · Density functional theory · Time-dependent DFT

1 Introduction

Quantum chemistry has nowadays reached a mature state allowing the treatment of molecular architectures that are relatively complex both in terms of size and nature. It has thus become an invaluable tool for the chemical understanding and some of its notions have spread allowing the entire chemists' community to benefit from its basic ideas and tools. Chemical concepts, such as "hardness" and "softness" [1,2] or even the idea, intrinsically related to molecular chemistry, of "bond" [3], have found a rigorous formulation in quantum chemistry thus allowing its use for the rationalisation and interpretation of reactivity and the properties of complex molecular systems [4].

Thanks to the development of embedding techniques [5–7] methods for the description of relativistic effects [8–10] and for the treatment of electron correlation [11,12] and new computer architectures and linearly scaling algorithms [13], large molecular systems can now be described by quantum methods with accuracy comparable of those of modern experimental techniques [14,15]. In particular, ab initio quantum methods are nowadays used not only to rationalise but also to predict several chemical phenomena. Remarkable examples in this field are the prediction of new chemical species [16, 17] or of gas-phase reactivity [18].

In the last decades, a key-role for the diffusion of quantum methods has been assumed by density functional theory (DFT) [19] which emerged as an invaluable tool for computation and analysis of the properties of large systems and especially for those containing transition metal atoms. DFT is an ab initio method solidly routed for the ground state relying, for practical applications, on an approximate expression of the exchange-correlation energy. DFT has a good scaling with the size of the system, it includes most of the correlation effects and it is monodeterminantal, thus allowing for an easy interpretation of the results in terms of molecular orbital analysis. For these reasons it has been successfully applied for the study of a wide variety of chemical systems [20].

Nevertheless, striking examples of DFT bias are well known: the incorrect description of the dissociation of two-center three-electron systems [21–23], the bad description of proton transfer barriers [24] and dispersion forces [25,26] or the overestimation of electron delocalisation [27,28] (affecting both magnetic [29] and structural properties [30]). These failures directly derive from the approximate nature of the functionals used and, in particular, from the local form of the exchange-correlation functionals [31], the lack of part of non-dynamical correlation [32,33] and the presence of the (spurious) contribution of self-interaction energy to the total energy [34–36]. In this context, it is not surprising that most of the methodological efforts in DFT development are currently devoted to seek new functionals/potentials solving

I. Ciofini
Ecole Nationale Supérieure de Chimie de Paris,
Laboratoire d'Electrochimie et Chimie Analytique,
CNRS UMR 7575, 11 rue P. et M. Curie,
F-75231 Paris Cedex 05, France
E-mail: ilaria-ciofini@enscp.fr

part (or, ideally, all) these problems. If for ground state properties a conscious user can safely use DFT or properly select other ab initio methods (Hartree–Fock or post-HF wavefunction approaches), the situation is more involved for the treatment of excited states [37]. Post-HF procedures can be used to accurately describe excited states [37–41]. They have the advantage of providing the intuitive picture of an excited state as the result of an excitation (or a linear combination of several excitations) from occupied to empty (virtual) orbital(s), but the disadvantage of a severe computational burden, especially when the whole set of occupied and virtual orbitals is included, that is when looking for the exact solution of the problem. Another possibility is to define an "active space" and to consider only excitations within the orbitals therein or select the "type" of excitation (only single, single and double etc.) of interest. Several techniques, either variational or perturbative, have been developed to solve these problems and they nowadays allow for the description of reasonably large molecular systems [42].

As in the case of DFT for the computation of ground state properties, the development of time dependent-density functional theory (TD-DFT) [43–45] supplied a valuable alternative to post-HF methods to study the excited state of large systems with reasonable accuracy. Although other approaches have been developed for the treatment of the excited states within the DFT formalism, such those of Ziegler [46] and Daul [47,48], the TD-DFT considers a formal extension of time independent DFT to cases where a time dependent external potential is applied. If we restrict ourselves to the inclusion of an external electric field, a variety of optical response properties, including UV/Vis absorption spectra, can be computed using the linear response theory and TD-DFT [43–45]. This latter has the great advantage of being computationally not very demanding and free of the bias introduced by the selection of a given reference space. More recently, the possibility to relax excited states within the TD-DFT formalism [49–52] has opened new horizons for the study of photochemically active systems since it allows the study not only of absorption phenomena but also of emission and of the reactivity at the excited state [53].

Nevertheless, there is still debate concerning the limits and the accuracy of TD-DFT calculations. First, some authors pointed out the "unreliability" of TD-DFT for the treatment of excited state involving charge separation, in particular charge transfer states [54–58] Rydberg states or excitation in highly conjugated systems [59–61]. In general, TD-DFT performs with accuracy for valence excited states while, in order to correct the underestimation of excitation energy for CT states obtained with standard TD-DFT methods, other techniques such as DFT-CI [62–64] or DFT/MRCI [65,66] have been proposed. Second, there is still an open question concerning the inclusion of high order excitations within this formalism [67–70]. All these problems are related to the approximations made within the TD-DFT formalism (such as the adiabatic local density approximation) and also to the approximate nature of the functionals used. In particular, and as already mentioned for the ground state, the local form of the functionals, the self interaction error, and, by consequence, their incorrect asymptotic behaviour, are the main sources of error in the calculations of the excited states [58,71–73]. Furthermore, functionals/potentials developed and tested only for ground state properties can be unreliable for the treatment of excited states. Only recently have the performance of several functionals for the calculation of excited states as well as basis set effect within the TD-DFT formalisms been systematically analysed both for reference organic molecules [74,75] and simple complexes containing transition metal ions [76], providing a suitable benchmark of TD-DFT capabilities. As a matter of fact, sticking to a pure TD-DFT approach, reasonable accuracy for interpretation and prediction of excited states of organometallic compounds can be achieved using hybrid functionals (i.e. those including a fraction of, exact, HF exchange) [58] or potential having the correct asymptotic behaviour (such as LB94) [71–73,77].

Still the calculation of excited states of supramolecular systems containing transition metal atoms represents a challenging perspective for all computational methods, including TD-DFT. The difficulties in predicting the excited states for such systems are not only related to their size but mainly to the very different natures of the excited states that have to be described with the *same* accuracy (such as d-d; metal-to-ligand-charge-transfer, MLCT; ligand-centred, LC; Rydberg states). If the large size of a system is due to the presence of bulky groups that play no role for the electronic properties of the systems, embedding techniques or even a crude modelling (i.e. study a smaller model systems) can be a suitable route without significantly altering the quality of the simulation. Nevertheless, if we are interested in the study of photochemical molecular devices (PMDs'), each part of the supramolecular system plays an important electronic role and its overall properties are the results of the interplay of each component and not simply their sum.

In the last years, there has been an increasing interest in the modelling and the synthesis of new PMDs. In particular, new, fairly sophisticated, supramolecular architectures [78, 79] able to selectively react to an external input and behaving as true devices at the molecular scale were designed and synthesised [80–84]. Amongst all the basic light-triggered processes, the most widely studied have been, by far, photoinduced electron transfers (PET) due to their prominent role in biological systems [85–87], and in the intermingled research fields of molecular electronics [78,79,88–109] and photochemical conversion (and storage) of solar energy [78, 79,89–93,109–113]. From an experimental point of view, when designing such functional model systems as prototype for artificial photosynthesis [114], one major aim is to create molecular assemblies favouring the formation of photoinduced long-lived charge-separated (CS) states [115]. These CS excited states actually correspond to the transient conversion of light into an electrochemical potential, which can be potentially used either for energy storage [110–114] or for electricity production [111–113,115–117].

To this end, specific PMDs were developed, generally referred to as *polyad*, where electron donating (D) and/or

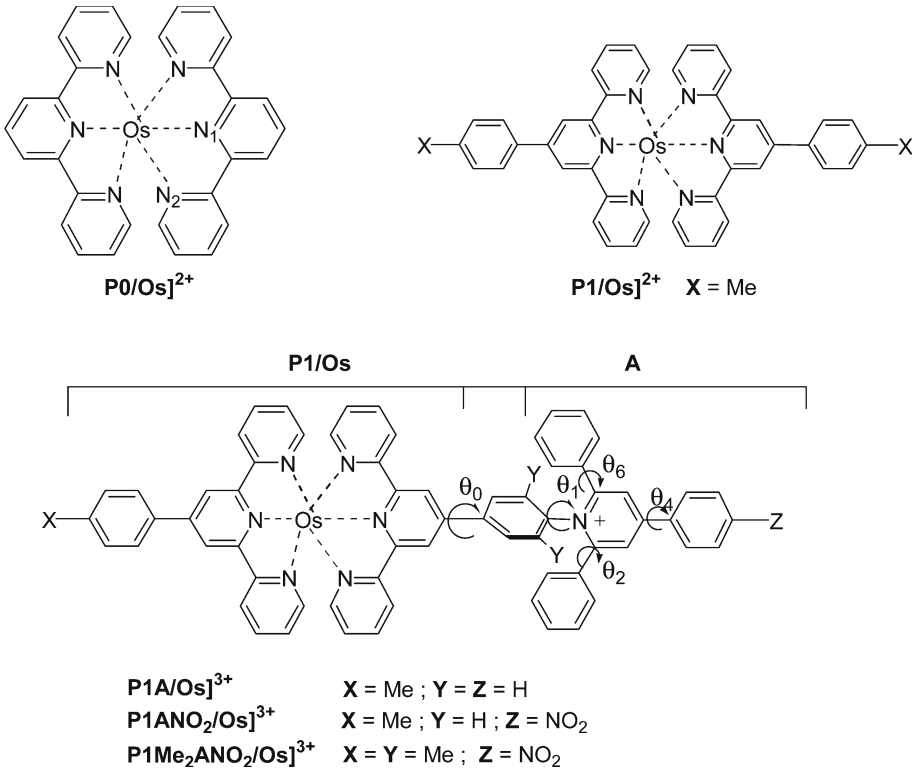

Fig. 1 Schematic representation and labelling of the Os(II) complexes analysed (M=Os)

accepting (A) units are connected together via a photosensitising component (P). Since, in such systems, each of the different units preserves its *functional* characteristics (here its electronic properties), they can be defined, within the conceptual framework of supramolecular photochemistry [91–93] as multicomponent systems. In this type of PMDs, the building blocks, normally arranged in a linear fashion [110] and following the D–P–A sequence, are usually held together by covalent links, hydrogen bonding or even only mechanical contacts [118,119]. The overall working mechanism of a resulting prototypical triad, D–P–A, is also experimentally relatively well settled [89–93,110,120,121]. After light excitation of the P unit (the primary donor), a cascade of intramolecular electron transfers takes place, leading to the lower-lying CS excited state, $*[D^+–P–A^-]$. This state should be employed before charge recombination (CR) occurs. Each of the different components of the polyads has been the subject of intense experimental design and synthetic work aimed at identifying and selecting the best P, A and D building blocks as well as proposing satisfactory intercomponent bridging units [78,79,89–93,120,121]. If the nature of the various functional components is now well established, still an intense activity [122] is going on to optimize them [123,124] and, especially, to adjust their electronic coupling [126–129].

In this paper we will consider two-components systems, that is *dyads*, of P–A type derived from the functionalisation of the $[Os(tpy)_2]^{2+}$ photosensitiser, **P0/Os** (tpy = 2,2′ : 6′, 2″-terpyridine, in Fig. 1), linked via a phenyl spacer to an electron-acceptor group (A) of the triphenylpyridinium $[H_3TP]^+$ type (**P1A/M**, see Fig. 1) [130–132]. More precisely, these dyads (**P1ANO$_2$** and **P1Me$_2$ANO$_2$**, Fig. 1) derive from a family of triarylpyridinio-functionalised [4′-(*p*–phenyl)$_n$]terpyridyl ligands, $R^1_2R^2TP^+$ -(p)$_n$tpy (here, R^1 = H, R^2 = NO_2, and n = 1) recently proposed [130–132], that has the advantage, when complexed, of being structurally rigid and, at the same time, chemically flexible (due to the possible R^1 and R^2 functionalisation). Therefore, the two major criteria required for an efficient charge separation (i.e. (a) a rod-like shape and (b) a controlled overall architecture) are fully satisfied by these dyads. Both factors allow to untimely avoid withdrawal of the molecule that could favour charge recombination (intramolecular "short circuit") [133]. Furthermore, the two bulky phenyl substituents ortho to the $N_{pyridinio}$ atom of the electron–acceptor group (A) should prevent the pyridinium ring from adopting a coplanar conformation with the covalently linked photosensitiser unit (P1) and warrant the disruption of the conjugation between the two connected subunits. This effect should be enhanced by the presence of the methyl groups on the phenyl spacer in the case of **P1Me$_2$ANO$_2$/Os** (Fig. 1). In other words, the necessary intercomponent *electronic decoupling* is expected to be produced by a *geometrical decoupling* [134], which is playing the role usually fulfilled by saturated spacers. Experimentally, the effectiveness of such a correlation between structure and electronic properties has been demonstrated in

the relaxed ground state for the acceptor-dyads in their native form, **P1A/M** [131,132]. Nonetheless, the behaviour of the electrochemically reduced forms, $[\mathbf{P1A/M}]^-$, to some extent mimicking the targeted CS state $[P^+–A^-]$, remained experimentally unclear [132]. A theoretical (DFT) study of the ground state properties of the various species both in their *native* and *reduced* forms (i.e. $[\mathbf{P1/M}]^-$ and $[\mathbf{P1A/M}]^-$), as well as their electronic absorption spectra was recently published [135].

This study [73] allowed establishing the important role played by the phenyl spacer in coupling the acceptor (A) and the photosensitiser (**P0/Os**) and, more generally, the importance of the intercomponent coupling on both the redox and photochemical processes taking place in the molecule. In particular, both from experimental and theoretical data, it's clear that the phenyl spacer is more strongly coupled to the **P0/Os** unit than to the acceptor: its presence strongly modifies the characteristic of the photosensitiser and basically creates a new photosensitiser unit (the **P1/Os**). Indeed, at the same time the phenyl spacer plays also the role of a connector between the **P1** unit and the acceptor. Therefore the new supramolecular device is better described as a *dyad* (**P1–A**), with peculiar characteristic due to the presence of the spacer, rather than a formal P0-phenyl-A triad.

Moreover, experimentally, electrochemical properties of P1 and A within P1–A as well as their absorption features, especially in the visible region (MLCT band) seem, at first sight, the same as those of the isolated components (P1 and A) [132]. From these data it was inferred that there is a presumably small coupling between the phenyl spacer belonging to P1 and the acceptor [132]. On the other hand, after reduction it was clearly shown that the dyads do not behave as the sum of the single components: the intercomponent coupling is present and plays a key role, ruling the properties of such systems [132,135]. A theoretical analysis [135] allowed identifying the origin of the coupling and also its hidden signature in the UV part of the absorption spectra, thus providing a complementary tool of analysis for the interpretation of the photophysical behaviour of such systems.

From a more technical point of view, since the properties are not simply additive, methods based on the classical "divide and conquer" idea (such as ONIOM) [5,6] or extreme simplifications of the structure cannot be applied to study the excited state properties of such systems. On the other hand, only a theoretical analysis of the properties of the supramolecular entity would allow, by comparison, to understand and to decompose the role of each of its constituting unit. For these reasons these dyads represent a good example of complexity in chemistry since, although relatively small compared to other functional systems (such as the biological ones, for instance), they can act as real devices. They are also a challenge to current ab-initio methods since they especially claim to be a method able to fully describe the supramolecular ground and excited state as a whole.

In this work, in order to asses the limits of validity of our computational procedure, based on the use of TD-DFT and a hybrid functional (PBE0) [136], we shall first study the properties of the simplest photosensitiser (**P0/Os**) for which experimental and computational studies are available in literature [137]. In this paper we shall limit our discussion to spin allowed transition (i.e. S_0–S_n) and therefore never discuss the spectral range ($\lambda > 650$ nm) where ^{3} MLCT transitions occur. The same protocol will be then applied to study the singlet excited states of the dyads (**P1ANO$_2$/Os** and **P1Me$_2$ANO$_2$**). Finally the properties of these systems after single electron reduction will be studied with the same protocol.

Our results clearly show the perspectives but also the limits of current DFT approaches: at the ground state they allow to evaluate the quality of DFT in the description of delocalised *vs* localised density through the evaluation of delocalisation on the π system. At the excited state they allow to judge TD-DFT on the description of complex systems.

DFT and TD-DFT provide a good qualitative description of these complex supramolecular architectures although some effects are still missing and the description is not fully quantitative. In particular, from what concerns the description of the excited states, all MLCT transitions are correctly described while higher excited states (in particular LC transitions) are poorly defined. The correct description of MLCT states using TD-DFT could seem to be in contradiction with previously reported studies on charge transfer excited states [54–58]. In this context it should be underlined that the MLCT bands considered here are still valence excitations and thus completely different in nature from the long range CT described in literature as failures of current TD-DFT [54–58].

On the other hand, in order to refine the description of PMDs, environmental effects should be taken into account both at intrinsic and explicit levels. In fact, especially for charged dyads such as the one under analysis, solvent as well as counter-ions are expected to play a major role both in the ground and in the excited states. These effects, normally neglected in the simulations, are indeed experimentally known to produce strong changes in the photochemical properties of these types of complexes, ranging from a blue shift of the emission from MLCT to the complete preclusion of the formation of CS in going from fluid to rigid media (see for instance reference [138].

The qualitative and quantitative agreement reached in the description of the photochemical properties of our PMD opens new frontiers for the application of computational methods for the interpretation and prediction of the properties and reactivity of these systems at the excited states. In particular, the ab initio modelling could guide the efficient design of new PMDs (highlighting the effect of metal or functionalisation of the molecular assemblies) but also offer an additional tool for the characterisation of excited states, very hard to observe from an experimental point of view

Finally it is worthwhile mentioning that the evolution of the PMDs towards photo-magnetic-molecular-devices (PMMDs) [139–143] would need to couple the description of their photochemical properties with other properties, such as magnetic exchange interactions, opening a completely new and extremely challenging experimental and theoretical field.

Table 1 Main structural features computed for Os(II) complexes

	P0/Os	**P1/Os**[b]	**P1A/Os**[b]	**P1ANO$_2$/Os**	**P1Me$_2$ANO$_2$/Os**
d(M–N$_2$)	2.066 (2.089[a])	2.066	2.069	2.069	2.069
d(M–N$_1$)	1.988 (1.972[a])	1.989	1.999	2.000	1.998
d(M–N$_{2(A)}$)[c]	–	–	2.063	2.063	2.063
d(M–N$_{1(A)}$)[c]	–	–	1.979	1.978	1.979
d(N$_{pyr}$–C)	–	–	1.458	1.461	1.465
θ_0	–	30.6	29.3	28.7	28.4
θ_{0A}	–	–	35.9	36.7	34.0
θ_1	–	–	67.3	67.7	76.4
θ_2	–	–	60.9	60.4	58.6
θ_6	–	–	56.3	60.4	58.6
θ_4	–	–	24.5	28.0	28.9
θ_{NO2}	–	–	–	0.3	0.5

Distances in Å, angles in degrees, experimental values in parenthesis
[a] From ref. [159]
[b] From ref. [135]
[c] Metal to nitrogen distance of the tpy carrying the acceptor

2 Computational methods

All calculations were carried out using a development version of the Gaussian code [144]. A hybrid Hartree–Fock/density functional model (HF/DFT), referred to as PBE0, was used [136]. This approach was obtained by casting the PBE exchange and correlation functional [145] in a hybrid DFT/HF scheme, where the HF/DFT exchange ratio is fixed a priori at 1/4 [146].

In the case of open shell systems, unrestricted calculations were performed and spin contamination, monitored by the expectation value of S^2, was found to be negligible.

A double ζ quality LANL2 basis [147], and corresponding pseudo-potentials for the metal atom (Os) [148], was used for all atoms both for the structural optimizations and the calculation of the electronic properties. Such a level of theory (DFT + LANL2DZ basis set) had previously been successfully applied in a few works concerning the structure, spectroscopic properties and reactivity of organometallic systems [135, 149].

The molecular structure of each compound was fully optimized: D_{2d} and C_2 symmetry constrains were imposed for the **P0/Os** and **P1/Os**, respectively, while all other systems were computed without symmetry constrains.

Optical transitions were computed using the TD-DFT at the same level of theory. Among all of electronic transitions calculated, only the ones having non-negligible oscillator strengths ($f > 0.01$) were reported in the tables while all transitions have been included in the simulations of the spectra. As described in [135], to have a direct comparison with the experimental data, the spectra were simulated using Gaussian functions, the only adjustable parameters being the full-width at half-maximum (*fwhm*), that is the broadening of each peak (individual transition). This broadening strongly, varies from one transition to another and, a fortiori from one system to another. At the same time, *experimental* absorption bands, like MLCTs, generally result from the sum of many and various transitions, thus making the *fwhm* parameters not directly attainable from experimental data. To circumvent these problems, a fixed bandwidth was used, the *fwhm* parameter being set at 0.15 eV.

In this paper only singlet–singlet (i.e. spin allowed) transitions will be discussed. The transitions were computed up to 220 nm for **P0/Os** and 337 nm for the dyads. When spin density is discussed we refer to Mulliken spin density.

3 Results and discussion

Density functional theory (DFT) has proven to provide reliable results in the prediction of the ground state properties of many organometallic systems including Ru(II) and Os(II) complexes with polypyridine ligands. In particular, the ground state geometrical properties of Os complexes with bpy (2, 2′-bipyridine) or tpy ligands have been already discussed in a number of papers [135, 137, 150–158] and here the results obtained at the PBE0 level of theory for the systems depicted in Fig. 1 will be only briefly summarised. For a more detailed analysis we refer to [135]. Selected optimised geometrical parameters are reported in Table 1. The metal, Os, is pseudo-octahedrally (D_{2d}) coordinated, with shorter M–N$_{tpy}$ bonds along the main axis (the one passing by the metal and the nitrogen atoms, N1, of the central pyridine ring of each tpy), in agreement with previous experimental findings. Bond lengths are in agreement with X-ray structure available [159] for P0/Os (2.089Å and 1.972Å experimental versus 2.066Å and 1.988Å computed, respectively). As expected, the functionalisation of the tpy barely affects the coordination sphere of the metal, the metal to nitrogen distances and angles being practically unchanged when going from **P0/Os** to **P1/Os** or to **P1A/Os** and derivatives (maximum variations 0.02Å, Table 1). All other geometrical features are very similar except the angle describing the torsion of the pyridinium ring with respect to the P1 unit (θ_1). In fact, as a consequence of the functionalisation on the phenyl spacer with bulk methyl groups in **P1Me$_2$ANO$_2$/Os**, θ_1 is increased by ca. 10°. The acceptor moiety (A) is therefore more orthogonal to the P1

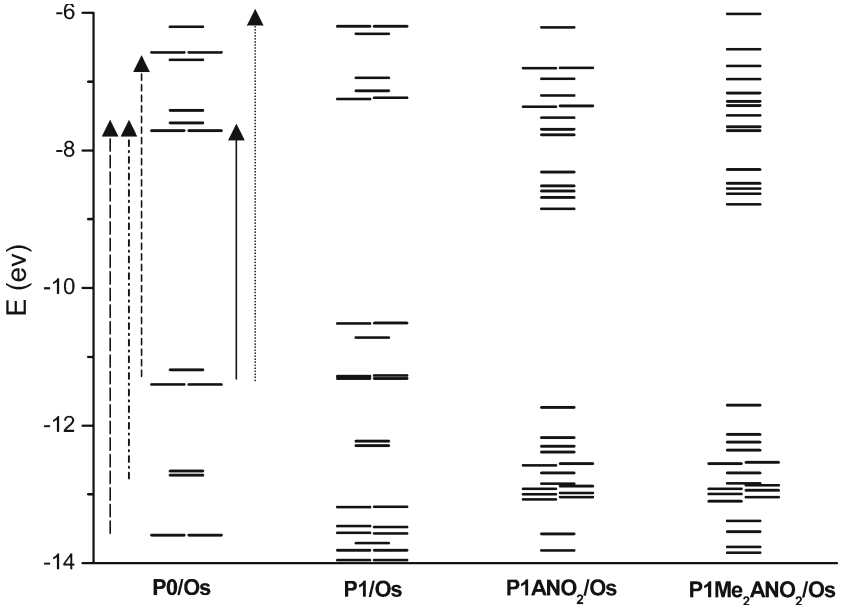

Fig. 2 Molecular Orbital energy diagrams computed for **P0/Os**, **P1/Os**, **P1ANO$_2$/Os** and **P1Me$_2$ANO$_2$/Os**

system and it is thus expected to be geometrically more decoupled from the photosensitiser as experimentally aimed.

From an electronic point of view, the typical molecular orbital splitting of a d^6 pseudo-octahedral metal complex is found for the **P0/Os** system (Fig. 2). The three highest occupied MO are of *d* character fully localized on the Os atom, while the lowest unoccupied MOs (LUMO and higher) are π^* orbitals centered on the ligands. A large energy gap between the occupied metal orbitals and the occupied π orbitals of the tpy (HOMO-3 and below) is computed. As soon as the phenyl spacer is introduced (**P1/Os**), a strong perturbation of the occupied metal *d* orbital is computed and their splitting no longer resembles that of the P0 system. First, all the occupied and virtual orbitals are shifted to higher energies as a consequence of the electron donor character of the terminal methyl. In fact, as experimentally already reported in literature [160], the phenyl behaves neither as an acceptor nor as a donor, but the methyl possesses a small donor character that is simply "transmitted" through the phenyl, the overall phenyl-CH_3 moiety acting as a donor [160]. Indeed, this effect is small and global and would not change the peculiar characteristic of the photosensitiser, the variation of the HOMO-LUMO gap being negligible (3.5 eV in **P0/Os** vs 3.3 eV in **P1/Os**). In fact the main consequence of the phenyl substitution in P1 is on the occupied orbitals. In particular, a splitting of the d manifold and a substantial mixing of the *d* occupied orbitals with orbitals centred on the phenyls is found in **P1/Os**. Since this complex is still C_2 symmetric, the same pseudo-degeneracy of **P0/Os** is present. The two pseudo-degenerate *d* orbitals strongly interact with two phenyl centred orbitals giving rise to the four orbitals with mixed *d*-phenyl character (HOMO–HOMO-1 and HOMO-3 – HOMO-4, respectively) while the non degenerate *d* orbital (HOMO-2) is practically unperturbed. Furthermore two other pseudo-degenerate and occupied orbitals completely localised on the phenyl spacer lie very closely to the *d* manifold (HOMO-5 and HOMO-6). These latter are well separated from the occupied π orbitals localised on the tpy (HOMO-6 and HOMO-7). The perturbation introduced in **P1/Os** by the presence of the phenyl group is signficant since, by altering the splitting of the *d* manifold, it is expected to yield a new photosensitiser unit. This is experimentally reflected by the different absorption and redox properties of P1 with respect to P0 and it has been already shown by previous calculations [135]. In other words, the phenyl is not simply a "substituent" on the tpy but strongly couples to the P0 unit giving rise to a new block, P1.

When the acceptor moiety is introduced to form the dyads (**P1ANO$_2$/Os** and **P1Me$_2$ANO$_2$/Os**) the molecular orbital splitting of the symmetric **P1/Os** complex is perturbed (refer to Fig. 2) mainly due to the removal of C_2 symmetry as a consequence of the asymmetric substitution. Indeed, the MO splitting looks very similar for both dyads, thus underlying the limited effect of the methyl group in the orbital diagram, in accordance with experiment [132].

The interaction between the ligand and the Os *d* orbitals is modified by the presence of the acceptor and the degeneracies of the *d* manifold are removed. The highest occupied molecular orbital still retains a *d* character but with a significant mixing of the phenyl of the ancillary tolyl–tpy: the other orbital that corresponds to the same type of interaction (*d*-phenyl of the ancillary tolyl–tpy) being the HOMO-5/HOMO-4 for **P1ANO$_2$/Os** and **P1Me$_2$ANO$_2$/Os**, respectively. The HOMO-1 correlates to the HOMO-2 of **P1/Os**, having mainly a *d* character with small mixing of π tpy orbitals, while the other *d* orbital, interacting with the tpy bearing the acceptor, is the HOMO-2. More generally, the introduction of the acceptor modifies the interaction of one of the ligands with the *d*-metal orbitals but does not completely

Table 2 Principal computed electronic transitions (in nm) and associated oscillator strength (f) computed for **P0/Os**, **P1ANO$_2$/Os** and **P1Me$_2$NO$_2$/Os**[a]

P0/Os			**P1ANO$_2$/Os**			**P1Me$_2$NO$_2$/Os**		
λ	f	Experimental[b]	λ	f	Experimental[b]	λ	f	Experimental[b]
535	0.02	MLCT 476.5 (1.74)	571	0.01	MLCT 491.7 (3.07)	567	0.01	MLCT 491.2 (3.27)
535	0.02		501	0.32		501	0.01	
430	0.03		500	0.01		501	0.34	
430	0.03		486	0.13		485	0.10	
427	0.21		466	0.02		466	0.02	
416	0.02		460	0.04		460	0.04	
416	0.02		435	0.4		436	0.37	
336	0.04	LC 312 (8.04)	369	0.08	MLCT/LC 393 *sh* (1.03) 313.7 (9.86) 290.5 *sh* (8.34)	370	0.03	MLCT/LC 398 *sh* (1.04) 313.7 (11.46) 289.5 *sh* (9.40)
331	0.03		368	0.01		367	0.01	
331	0.03		353	0.01		350	0.16	
328	0.02		350	0.22		346	0.01	
328	0.02		350	0.09		342	0.13	
316	0.04		349	0.05		341	0.07	
293	0.18		340	0.56		340	0.57	
293	0.18		340	0.06		336	0.30	
288	0.36					335	0.03	
288	0.36					335	0.02	
274	0.01							
268	0.02							
268	0.02							
265	0.06							
249	0.2							
235	0.4							
235	0.1							
235	0.1							
233	0.08							
232	0.07							
232	0.07							
228	0.06							
228	0.06							
221	0.04							
219	0.06							
219	0.06							

[a] Each component of E degenerate states is separately reported
[b] from P. Lainé (private communication) ϵ values in $10^{-4} \times M^{-1}cm^{-1}$ are given in parenthesis.

change the character of the photosensitiser thus allowing to formally recognise a P1 unit even when embedded within the dyad. Indeed, the gap between the occupied metal centred and ligand centred orbitals is strongly reduced, a purely phenyl centred (HOMO-3) and acceptor HOMO-4/HOMO-5 (for **P1ANO$_2$/Os** and **P1Me$_2$ANO$_2$/Os**, respectively) orbital lying very close to the MOs with substantial d metal character. Furthermore, between the purely tpy centred occupied π orbitals and the metal ones, a packet of closely lying orbitals with dominant contribution of orbitals located on the acceptor, either on the pyridinium ring or on the NO_2 moiety, can be found for both dyads. The same holds for the unoccupied orbitals where a packet of acceptor centred orbitals is found between the first $\pi*$ orbitals centred on tpy (computed at ~ -9 eV) and the ones higher in energy (computed at ~ -6 eV). Indeed, in both dyads the LUMO remains mainly centred on the tpy with a small contribution of the metal as in **P1/Os**, thus meaning that the acceptor used as electron withdrawing moiety is not strong enough to completely change the nature of the first excited states that will be, for all systems, an MLCT band involving the $\pi*$ orbitals of tpy as for **P1/Os**. Nevertheless, in the dyads the LUMO is no more symmetrically distributed over the two tpy but localized on the tpy bearing the acceptor. The first virtual molecular orbital fully localized on the pyridinium ring of the acceptor (LUMO+3 in both dyads) is computed to be higher in energy, ~ 0.3 eV above the LUMO.

Furthermore, a global consequence of the presence of the acceptor, when going from the **P1/Os** complex to the dyads, is an overall shift of the orbitals to lower energies but also a reduction of the HOMO–LUMO gap from 3.3 eV, computed for **P1/Os**, to 2.9 eV for the dyads, due mainly to a significant lowering of the LUMO energy. Therefore, for the latter systems, we can expect the MLCT band to occur at slightly lower energies.

More generally, comparing P0, P1 and the dyads, we can see that the introduction of the phenyl increases the metal to ligand interaction while the asymmetric acceptor slightly alters the d splitting and mostly provides a packet of closely lying occupied and empty acceptor centered orbitals that can be involved in MLCT of LC transitions at lower energy than those occurring in the native **P1/Os** compound. As a

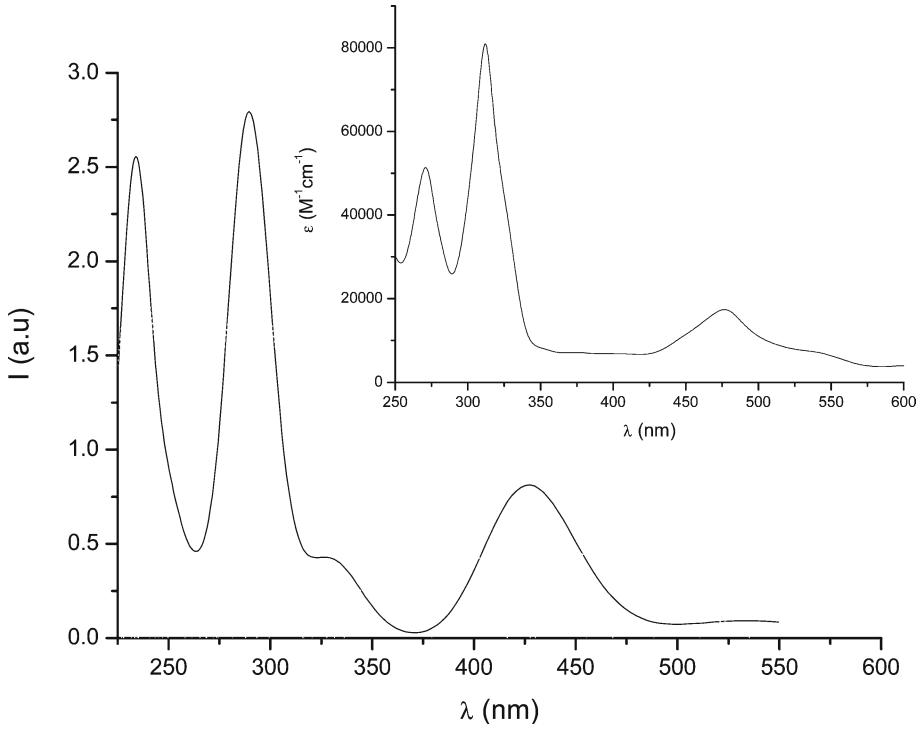

Fig. 3 Simulated spectra of **P0/Os**. Inset: experimental spectra

consequence we can expect that, for the dyads, several π or π^* orbitals could contribute to the same MLCT or LC transition.

In summary, the analysis of the molecular orbitals of P0, P1 and P1A derivatives, allowed us to recognise the importance of the phenyl spacer in modifying the properties of the photosensitiser core but also to provide a channel for inter-component coupling

3.1 Excited state properties: UV/Vis absorption spectra

The main singlet–singlet transitions computed for **P0/Os** are reported in Table 2 and the corresponding simulated spectrum is plotted in Figure 3. The computed spectrum consists of three intense bands: the first, with absorption maximum at 429 nm (symmetric), a second one at 290 nm with a shoulder at 326 nm and a third one, higher in energy and roughly symmetric, computed at 233 nm. The first band is, as expected, due to metal-to-ligand-charge-transfer transitions (MLCT) involving the three Os d metal orbitals (HOMO, HOMO-1 and HOMO-2) and the first four (empty) ligand centred π^* orbitals (full line arrow in the Fig. 2). The dominant transition within this band is of B_2 symmetry and it is computed at 427 nm ($f = 0.21$). Other ancillary transitions, of E symmetry, are computed at 430 and 416 nm with lower intensity ($f = 0.03$ and $f = 0.02$, respectively). Actually another MCLT transition is computed at 535 nm but due to its small intensity ($f = 0.02$) it is most probably covered by the ^{3}MLCT bands expected to occur in the same spectral region and not computed in this contribution. The second intense band, simulated at 290 nm can be assigned as a ligand-centred (LC) since the transitions contributing with highest intensity (computed at 293 and 288 nm) are essentially tpy centred π–$\pi*$. In fact, they correspond to excitations from the highest set of occupied π orbitals of tpy (HOMO-3 and HOMO-4) to the first set of virtual (π^*) orbitals of tpy (LUMO and LUMO+1). These excitations are schematically represented by the dash-dot arrow in Fig. 2. Indeed the band at 290 nm covers also two other lower intensity transitions having an MLCT character and computed at 328 and 316 nm ($f = 0.02$ and $f = 0.04$). These latter, represented by the dashed arrow in Fig. 2, involve excitations from Os occupied d orbitals to $\pi*$ orbitals of tpy higher in energy (LUMO+5 to LUMO+7). This set of transitions build up the shoulder of the band computed at 290 nm, which can be easily recognized in the simulated spectrum at 326 nm (Fig. 3), and is the main cause of the overall asymmetric band shape.

Finally two transitions mainly contribute to the band with absorption maximum simulated at 233 nm: one at 249 nm and one at 235 nm. Both transitions have mainly an LC character (corresponding to π–$\pi*$ excitations, long dash arrow in Fig. 2) although sizable d to $\pi*$ contributions (i.e. MLCT, dotter arrow in Fig. 2) are found, the MLCT contribution being larger for the first transition (i.e. that computed at 249 nm). More generally, as soon as the excitation energy increases, the excited states are better described by linear combinations of one electron excitations. Consequently it becomes quite difficult to assign a single, leading, excitation for each transition and the approximations done at TD-DFT level become more severe. Nevertheless, the overall character of the transitions

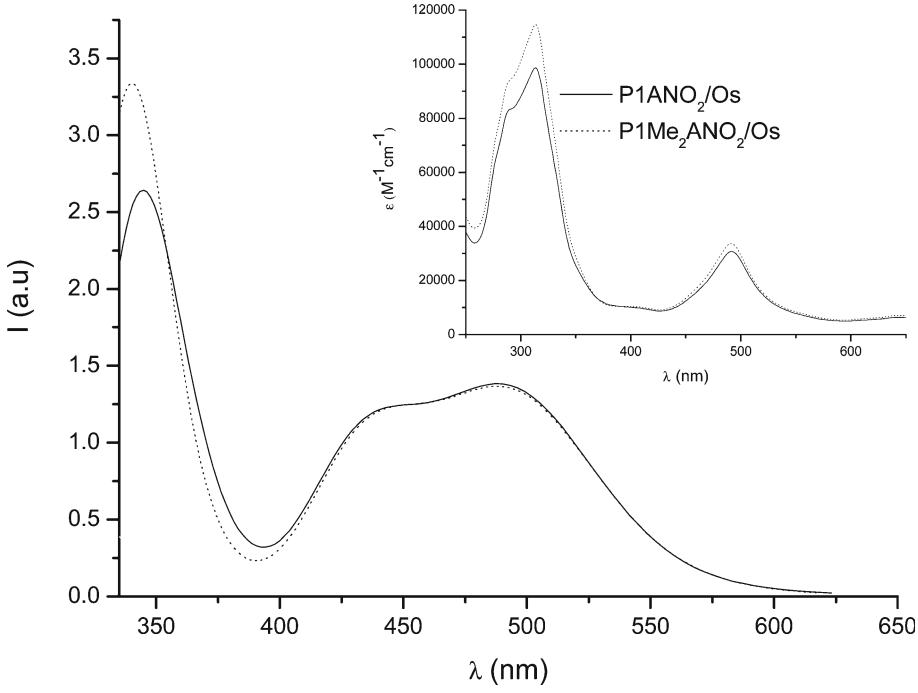

Fig. 4 Simulated spectra of **P1ANO$_2$/Os** and **P1Me$_2$ANO$_2$/Os**. Inset: experimental spectra

and of the resulting simulated bands (MLCT or LC) can still be clearly defined. When comparing with the available experimental spectra (P. Lainé, private communication) we can note that the calculated transition energies are systematically overestimated by ca. 0.3 eV for both the MLCT and the LC band. In fact, the MLCT band is experimentally found at 476.5 nm and predicted at 425 nm, while the LC one is found at 312 nm and predicted at 290 nm. Our results are in line with other TD-DFT calculations of **P0/Os** reported in literature using a comparable approach (in particular, a hybrid functional) [137].

The introduction of the phenyl spacer and acceptor moiety on the tpy ligand induces significant changes in the absorption spectrum of both dyads (**P1ANO$_2$/Os** and **P1Me$_2$ ANO$_2$/Os**) respect to that of **P0/Os**. Comparing with the computed transitions of **P0/Os**, Table 2, it can be noticed that all excitations are shifted to lower energies, in agreement with the smaller HOMO–LUMO gap and *d*-orbital splitting induced by the presence of the phenyl spacer (i.e. the change of the photosensitizer unit from **P0** to **P1** refers to the previous section and to the orbital splitting diagram in Fig. 2).

The simulated spectra of **P1ANO$_2$/Os** and **P1Me$_2$ANO$_2$ /Os**, reported in Fig. 4, are almost identical, in agreement with the experimental findings (P. Lainé, private communication). They consist of two main bands: the first, calculated in the 420–510 nm region, is very broad and asymmetric while the second computed around 350 nm is much sharper and symmetric. While the first band is practically unperturbed by the introduction of the methyl groups on the phenyl spacer, the latter is found to gain intensity in the case for **P1Me$_2$ANO$_2$/Os**.

Analysing the character of the excitations involved, the first band can clearly be assigned to MLCT transition while the second includes both LC and MLCT transitions. Two main MLCT transitions, computed at 501 and 435 nm for **P1ANO$_2$/Os** and at 501 and 436 nm for **P1ANO$_2$/Os** and at 501 nm and 436 nm for **P1Me$_2$ANO$_2$/Os**, and several ancillary ones contribute to the first band, thus determining its broad and asymmetric shape. These transitions, as in the case of **P0/Os** and **P1/Os**, involve excitations from the orbitals with substantial *d* metal character (HOMO, HOMO-1, HOMO-2 and HOMO-5/HOMO-4 for **P1ANO$_2$/Os** and **P1Me$_2$ANO$_2$/Os**, respectively) to the first five (empty) ligand centred π^* orbitals (LUMO, LUMO+4). None of the most intense ones has a dominant contribution corresponding to the direct optical electron transfer from the metal to the acceptor (that is an excitation from a d centred to the LUMO+3). This type of excitation, corresponding to the formation of a truly charge separated state by optical ET, is found to occur at higher energy (respectively at 369 nm for **P1ANO$_2$/Os** and 370 nm for **P1Me$_2$ANO$_2$/Os**) and it is practically hidden by the more intense MLCT and LC transitions occurring in the same spectral region.

The most intense transition for the dyads ($f = 0.56$) is computed at 340 nm and corresponds to one electron excitations of MLCT and LC (acceptor centred) characters. Another intense transition of MLCT type is computed, for both species, at 350 nm ($f = 0.22$ and $f = 016$). Only in the case of **P1ANO$_2$/Os** two other acceptor-centred transitions are computed at 341 nm ($f = 0.13$) and 336 nm ($f = 0.30$) thus, in agreement with the experiment, determining the higher absorption of the methyl functionalised dyad (**P1Me$_2$NO$_2$/Os**)

Table 3 Computed spin density (Mulliken, in %) for the relaxed ground state of various Os(II) complexes in their reduced forms

	$[P0/Os]^-$	$[P1/Os]^-$	$[P1A/Os]^-$	$[P1ANO_2/Os]^-$	$[P1Me_2ANO_2/Os]^-$
Os	0.08	2.8	12.6	11.0	10.9
tpy_A	2×49.96	2×46	72	56	62
ϕ_S	–	2×2	8	9	6
L1	**–**	**2×48**	**80**	**65**	**68**
pyridinium	–	–	5	18	16
ϕ_4	–	–	0.6	4	2.4
NO_2	–	–	0	1	1
A	**–**	**–**	**7.4**	**23**	**19**

in this region. Unfortunately, due to the size of the systems, the transitions for the dyads were computed up to 337 nm only. It is therefore likely that more intense LC transitions (both $\pi \rightarrow \pi^*$ centred on tpy or fully acceptor centred) occur at slightly higher energy and contribute to the band experimentally found at 309 nm. In other words most probably the LC and MLCT transitions computed in the 370–340 nm region are only a part of LC excitations observed in the spectra. For these reasons it is not possible to compare the shift in LC $\pi \rightarrow \pi^*$ computed for the dyads with those computed for the parent **P1/Os** complex. The overall agreement with the experimental spectra for the MLCT bands is similar to that obtained for **P0** and **P1**.

More generally, the presence of the acceptor influences the spectra of the system by lowering the symmetry. As a result of the combined influence of the terminal electron donating methyl substituent (mainly destabilising the HOMO) and of its electron acceptor unit, $[H_3TP]^+$ (mainly stabilising the LUMO), the HOMO–LUMO gap is smaller within the dyads than with respect to the parent homoleptic (symmetric) P1 and P0. Thus, all the transitions are shifted to lower energies. Furthermore it should be stressed that the direct optical electron transfer is computed to be of weak intensity with respect both to the LC and MLCT bands. Thus, the overall spectra can be considered as the superposition of the spectra of the single component (A and P1) only at first order since evidences of intercomponent electronic coupling of the units are hidden in the absorption spectra (in the UV range). Indeed, from the experimental analysis of the spectra (and in particular of the MLCT band) no clear evidence of coupling could be directly derived simply because the presence of an acceptor does not significantly change either the LUMO or the *d* manifold splitting with respect to P1. *This is a further proof of how a correct interplay between theory and experiment could help in the elucidation of hidden phenomena.*

3.2 MLCT as light induced redox-charge separated state

A possible way of describing MLCT transitions is to consider them as the results of a light-triggered intramolecular redox reaction: the metal center is oxidized while ligands are reduced to create an excited $*[M^+ –L]^-$ species [89,90,161, 162]. Previous experimental findings reported in the literature in the case of Ru/Os oligopyridine complexes show that the MLCT excited state show the same photo-excited electron reactivity of the ground state of related mono-reduced species [161]. In fact, for the type of systems we are interested in, the reduction is known to be essentially a ligand-centred process [89,90,161] although it is clear that reorganisation of the around the metal centre is not completely negligible.

Experimentally the approach outlined above is well known and it consists in performing spectro-electrochemical experiments: the electronic absorption spectrum of a system is recorded when applying a fixed external potential corresponding its one electron reduction (here of the acceptor). Basically, with this kind of method we simulate the excited state, $*[P1^+ –A^-]$, of a (N electrons) system by analysing the ground state of the corresponding reduced ($N + 1$ electrons) system $[P1–A^-]$.

From a computational point of view, a straightforward way to investigate the nature of the reduced species and, therefore, to compare with the results of spectro-electrochemical experiments, is to consider the spin density distribution calculated for the mono-reduced species [135,161,162]. An alternative approach would be to analyze the (Single occupied MO SOMO) but in the latter case spin polarisation effects would not be taken into account. The computed spin densities of all mono-reduced species are collected in Table 3. In all cases, all structures of the systems were relaxed for the reduced form.

The main outcomes concerning the computed mono-reduced complexes are the following:

1. For **P0/Os**, the reduction is completely centred on tpy.
2. For **P1/Os**, the reduction is centred on tpy with only a very small contribution on the dangling phenyl spacer
3. For the dyads, the reduction is no more clearly centered on the tpy ligand as the first reduction process is no longer assumed to occur on the photosensitiser but on the acceptor group.

Indeed, as already found for the **P1A/Os** systems [135], the spin density is almost completely localised on the ligand bearing the acceptor but with a substantial contribution of the tpy moiety (56 and 62%, respectively). Only a smaller contribution is computed on the pyridinium itself (18 and 16%, respectively, Table 3). Almost no spin density is found on the NO_2 while a non-negligible spin density is computed on the phenyl spacer connecting the acceptor moiety to the tpy (ϕs in Table 3). Lastly, a sizable amount of spin density is found on the metal center (up to 11%).

All these evidences are consistent with a description of the reduction of **P1ANO$_2$/Os** and **P1Me$_2$ANO$_2$/Os** as mainly consisting in a reduction of the acceptor moiety associated with a sizable – unexpected – reduction of the chromophore as a consequence of an intramolecular charge redistribution. The localisation on the acceptor is enhanced by the presence of NO_2 but only slightly perturbed by the presence of the Me groups borne by the spacer. It is clear from the computed structural data that these Me groups induce a geometrical decoupling (both in the native and reduced forms) by increasing the θ_1 dihedral and, as a consequence, results in an electronic decoupling. Nevertheless, besides their geometrical effect, another possible contribution of the two methyl groups – at the electronic level – stems from their inductive effect that compensates part of the electronic decoupling, thus the net results on spin density is negligible.

All these issues are in accordance with the experimental data and computations [132,135] previously reported for the [**P1A/Os**]$^-$ reduced . Indeed, it was shown that this species displays the spectroscopic signatures of both the reduced acceptor and the reduced chromophore [**P1/Os**]$^-$ [132,135]. Therefore, even if the acceptor moiety retains almost entirely its properties within the native dyad system, part of the spin density is transferred back from the reduced acceptor to the metal centre through the phenyl spacer within [**P1A/Os**]$^-$. This fact points to the difficulty of clearly defining the role of the phenyl in the whole process. The phenyl is not only a *simple spacer* within the supramolecular system but takes an active part as a full bridging component in the electronic communication. Moreover it has been shown that, in the case of **P1A/Os**, the electronic properties (spectrum) of reduced **P1A/Os** cannot be simply considered as the sum of those of reduced acceptor and chromophore thus underlying the important role of geometrical and electronic coupling [132, 135].

4 Conclusion

In conclusion, the analysis of the photochemical properties of the PMDs clearly shows that the properties of these supramolecular architectures cannot be simply derived from the sum of the related isolated parent components. In other words, in these systems, there is an "emergence" [163]: The term "emergence" refers to the existence of a key novel feature (property) that arises in the supermolecule and it is not present in its isolated components therefore making it unpredictable.

These systems are the prototype of "complex systems" here mostly meaning not easy to separate in their basic buildings block, and very challenging both in experiment and theory.

For improving these PMDs and continuing within the DFT framework, it would be necessary to solve or at least correct for the wrong asymptotic behaviour of the functionals in order to get more trustful energies for higher excitations. Next, even if we have the theoretical tools needed to fully describe the supramolecular entity both at the ground and the excited states (that is unfortunately not yet the case although reasonable accuracy can be obtained with approaches such as the one here outlined), there are still several effects that are missing: solvent (either implicit or explicit) and counterions effects, spin orbit coupling (explicitly) and the relaxation of the excited states, amongst others. Once these effects are properly treated by first principle methods, our theoretical tools will be truly suitable for the challenging investigation of *real* molecular devices, helping and guiding their synthesis and functionalisation using "first principles"

Acknowledgements I am indebted to Prof. Carlo Adamo (ENSCP, Paris), Dr. Philippe Lainé (Université Paris V, Paris), Prof. Claude Daul (Université de Fribourg, CH) and Dr. Gaston Berthier (MNHN, Paris) for several enjoyable and fruitful discussions. Prof. Carlo Adamo and Dr. Philippe Lainé are also acknowledged for the time they spent in reading the manuscript. The "Institut de Développement et Ressources en Informatique Scientifique" (IDRIS, Orsay) and the "Centre Informatique National de l'enseignement Supérieur" (CINES, Montpellier) are acknowledged for allocation of computer time (projects 05173 and eca2508, respectively).

References

1. Geerlings P, De Proft F, Langenaeker W (2003) Chem Rev 103:1793
2. Chermette H (1999) J Comp Chem 20:129
3. Bader RFW (1990) In: Atoms in molecules – a quantum theory, Oxford University Press, Oxford
4. Koch W, Holthausen M (2001) In: A chemist's guide to density functional theory, 2nd edn. Weinheim,Wiley-VCH, New York
5. Vreven T, Morokuma K (2000) J Chem Phys 113:2969
6. Vreven T, Morokuma K (2000) J Comp Chem 21:1419
7. Casassa S, Pisani C (1995) Phys Rev B 51:7805
8. van Lenthe E (1996) The ZORA equation. PhD Dissertation, Vrije Universiteit, Amsterdam
9. Douglas M, Kroll NM (1974) Ann Phys 82:89
10. Jansen G, Hess BA (1989) Phys Rev A 39:6016
11. Andersson K, Roos BO (1995) In:Yarkony DR (ed) Modern electron structure theory, advanced series in physical chemistry, Singapore, World Scientific, Singapore
12. Werner HJ (1988) In: Lawley KP (ed) Ab initio methods in quantum chemistry Part II, Advances in Chemical Physics, vol 69. Wiley-Interscience, Chichester
13. Grotendorst J (ed) (2000) Modern methods and algorithms of quantum chemistry proceedings, 2nd edn. NIC Series vol 3. Forschungszentrum Jülich
14. Cramer CJ (2002) In: Essential in computational chemistry, theory and models, Wiley, New York
15. Jensen F (2002) In: Introduction to computational chemistry, Wiley, New York
16. Gagliardi L, Pyykkö P (2003) Inorg Chem 42:3074
17. Straka M, Pyykkö P (2003) Inorg Chem 42:8241
18. Mercero JM, Matxain JM, Lopez X, York DM, Largo A, Eriksson LA, Ugalde JM (2005) Int J Mass Spect 240:37
19. Parr RG, Yang W (1989) In: Density-functional theory of atoms and molecules (International Series of Monographs on Chemistry, No 16), Oxford University Press, Oxford
20. Chong DP (ed) (1995) Recent advances in density functional methods, World Scientific Singapore
21. Sastry NG, Bally T (1997) J Phys Chem A 101:7923
22. Chermette H, Ciofini I, Mariotti F, Daul CA (2001) J Chem Phys 114:1447
23. Chermette H, Ciofini I, Mariotti F, Daul CA (2001) J Chem Phys 115:11068
24. Adamo C, Barone V (1996) J Chem Phys 105:11007

25. Zhang Y, Pan W, Yang W (1997) J Chem Phys 107:7921
26. Tao J, Perdew J (2005) J Chem Phys 122:114102
27. Zhang Y, Yang W (1998) J Chem Phys 109:2604
28. Ciofini I, Adamo C, Illas F (2004) J Chem Phys 120:3811
29. Ciofini I, Daul CA (2003) Coord Chem Rev 238:183
30. Jacquemin D, Perpète EA, Ciofini I, Adamo C (2005) Chem Phys Lett 405:376
31. Martin RL, Illas F (1997) Phys Rev Lett 79:1539
32. Savin A (1996) In: Seminario JM (ed) Recent developments and applications of modern density functional theory, Elsevier, Amsterdam, p. 32
33. Gräfenstein J, Cremer D (2005) Mol Phys 103:279
34. Perdew JP, Zunger A (1981) Phys Rev B 23:5048
35. Ciofini I, Chermette H, Adamo C (2003) Chem Phys Lett 380:12
36. Ciofini I, Adamo C, Chermette H (2005) Phys Chem 309:6
37. Chantal D (2003) Coord Chem Rev 238:143
38. Roos BO, Seigbahn PEM (1977) The direct configuration interaction method from molecular integrals. Methods of electronic structure theory, Plenum Press, New York
39. Roos BO (1983) The multiconfigurational (MC) SCF method. In: Reidel D (ed) Methods in computational physics, D. Reidel publishing company, Dordrecht
40. Stanton JF, Bartlett RJ (1993) J Chem Phys 98:9335
41. Nakatsuji H (1979) Chem Phys Lett 67:334
42. Turki M, Daniel C, Záliš S, Vlček JrA, van Slageren J, Stufkens DJ (2001) J Am Chem Soc 123:11431
43. Gross EUK, Dobson JF, Petersilka M (1996) In: Nalewajski RF (ed) Denisty functional theory II, Springer, Berlin Heidelberg New York
44. Casida ME (1995) In: Chong DP (ed) Recent advances in density functional methods: Part I, World Scientific, Singapore
45. Singh R, Deb BM (1999) Phys Reports 311:47
46. Ziegler T, Rauk A, Baerends EJ (1977) Theor Chim Acta 43:261
47. Daul CA (1994) Int J Quantum Chem 5:867
48. Atanasov M, Daul CA, Rauzy C (2003) Chem Phys Lett 367:737
49. Van Caille C, Amos RD (1999) Chem Phys Lett 308:249
50. Van Caille C, Amos RD (2000) Chem Phys Lett 317:159
51. Hutter J (2003) J Chem Phys 118:3928
52. Furche F, Ahlrichs R (2002) J Chem Phys 117:7433
53. Rappoport D, Furche F (2004) J Am Chem Soc 126:1277
54. Casida ME, Gutierrez F, Guan J, Gadea FX, Salahub DR, Daudey JP (2000) J Chem Phys 113:7062
55. Sobolewski AL, Domke W (2003) Chem Phys 294:73
56. Tozer DJ, Amos RD, Handy NC, Roos BJ, Serrano-Andres L (1999) Mol Phys 97:859
57. Drew A, Fleming GR, Head-Gordon M (2003) Phys Chem Chem Phys 5:3247
58. Drew A, Weisman JL, Head-Gordon M (2003) J Chem Phys 119:2943
59. Drew A, Head-Gordon M (2004) J Am Chem Soc 126:4007
60. Casida ME, Jamorski C, Casida KC, Salahub DR (1998) J Chem Phys 108:4439
61. Tozer DJ, Handy NC (1998) J Chem Phys 109:10180
62. Parusel ABJ, Köhler G, Grimme S (1998) J Phys Chem A 102:6297
63. Parusel ABJ, Ghosh A (2000) J Phys Chem A 104:2504
64. Grimme S (1996) Chem Phys Lett 259:128
65. Grimme S, Waletzke M (1999) J Chem Phys 111:5645
66. Parusel ABJ, Grimme S (2001) J Phorphyrins Phthalocyanins 5:225
67. Casida ME (2005) J Chem Phys 122:54111
68. Maitra NT, Zhang F, Cave RJ, Burke K (2004) J Chem Phys 120:5932
69. Hsu C, Hirata S, Head-Gordon M (2001) J Phys Chem A 105:451
70. Hirata S, Head-Gordon M (1999) Chem Phys Lett 302:375
71. Casida ME, Casida KC, Salahub (1998) Int J Quantum Chem 70:933
72. Casida ME, Salahub DR (2000) J Chem Phys 113:8918
73. Grimme S, Parac M (2003) Chem Phys Chem 4:292
74. Stratmann RE, Scuseria GE, Frisch MJ (1998) J Chem Phys 109:8218
75. Adamo C, Scuseria GE, Barone V (1999) J Chem Phys 111:2889
76. Baerends EJ, Ricciardi G, Rosa A, van Gisbergen SJA (2002) Coord Chem Rev 230:5
77. Van Leeuwen R, Baerends JE (1994) Phys Rev A 49:2421
78. Lehn JM (1990) Angew Chem Int Ed. 29:1304
79. Lehn JM (1988) Angew Chem Int Ed 27:89
80. Grabowski ZR, Rotkiewicz K, Rettig W (2003) Chem Rev 103:3899 (conformation)
81. Cattani-Scholz A, Renner C, Cabrele C, Behrendt R, Oesterhelt D, Moroder L (2002) Angew Chem Int Ed 41:289 (isomerization/folding)
82. Rack JJ, Winkler JR, Gray HB (2001) J Am Chem Soc 123:2432
83. Schofield ER, Collin JP, Gruber N, Sauvage JP (2003) Chem Commun January 21(2):188 (motion)
84. Brouwer AM, Frochot C, Gatti FG, Leigh DA, Mottier L, Paolucci F, Roffia S, Wurpel GWH (2001) Science 291:2124 (shuttling)
85. Krauß N (2003) Curr Opin Chem Biol 7:540
86. Willner I, Willner B (2003) Coord Chem Rev 245:139
87. Lubitz W, Lendzian F, Bittl R (2002) Acc Chem Res 35:313
88. Aviram A, Ratner MA (1974) Chem Phys Lett 29:277
89. Juris A, Balzani V, Barigelletti F, Campagna S, Belser P, Von Zelewsky A (1988) Coord Chem Rev 84:85
90. Meyer TJ (1989) Acc Chem Res 22:163
91. Balzani V, Juris A, Venturi M, Campagna S, Serroni S (1996) Chem Rev 96:759
92. Balzani V, Scandola F (1991) Supramolecular Photochemistry, Ellis Horwood, Chichester
93. Balzani V, Moggi L, Scandola F (1987) In: Balzani V (ed) Supramolecular photochemistry, D. Reidel, Dordrecht, The Netherlands
94. De Silva AP, McClenaghan ND (2004) Chem Eur J 10:574 (and references therein)
95. Kawai T, Iseda T, Irie M (2004) Chem Commun January 7(1):72
96. Ballardini R, Balzani V, Clemente-León M, Credi A, Gandolfi MT, Ishow E, Perkins J, Stoddart JF, Tseng HR, Wenger S (2002) J Am Chem Soc 124:12786 (and references therein)
97. Irie M (2000) Chem Rev 100:1683 (optical/photochromism)
98. Feringa BL (2001) Acc Chem Res 34:504 (chiroptical)
99. Wenger OS, Henling LM, Day MW, Winkler JR, Gray HB (2004) Inorg. Chem 43:2043 (photochemical/luminescence)
100. Miura T, Urano Y, Tanaka K, Nagano T, Ohkubo K, Fukuzumi S (2003) J Am Chem Soc 125:8666 (photochemical/luminescence)
101. Coe BJ (1999) Chem Eur J 5:2464 (NLO)
102. Mitchell RH, Ward RT, Chen Y, Wang Y, Weerawarna SA, Dibble PW, Marsella MJ, Almutairi A, Wang ZQ (2003) J Am Chem Soc 125:2974 (electrochemical)
103. Andersson M, Sinks LE, Hayes RT, Zhao Y, Wasielewski MR (2003) Angew Chem Int Ed 42:3139 (electron transport)
104. Sato O (2003) Acc Chem Res 36:692 (magnetism)
105. Launay JP (ed) (1991) New J Chem 15 (special issue)
106. Hagfeldt A, Grätzel M (1995) Chem Rev 95:49
107. Bard AJ, Fox MA (1995) Acc Chem Res 28:141
108. Paddon-Row MN (1994) Acc Chem Res 27:18
109. Wasielewsky MR (1992) Chem Rev 92:435
110. Baranoff E, Collin JP, Flamigni L, Sauvage JP (2004) Chem Soc Rev 33:147
111. Hagfeldt A, Grätzel M (2000) Acc Chem Res 33:269
112. Bignozzi CA, Argazzi R, Indelli MT, Scandola F (1994) Sol Energy Mater Sol Cells 32:229
113. O'Regan B, Grätzel M (1991) Nature 353:737
114. Sun L, Hammarström L, Åkermark B, Styring S (2001) Coord Chem Rev 30:36
115. Hammarström L (2003) Curr Opin Chem Biol 7:666
116. Hirata N, Lagref JJ, Palomares EJ, Durrant JR, Nazeeruddin MK, Grätzel M, Di Censo D (2004) Chem Eur J 10:595 (and references therein)
117. Loi MA, Denk P, Hoppe H, Neugebauer H, Winder C, Meissner D, Brabec C, Sariciftci NS, Gouloumis A, Vázquez P, Torres T (2003) J Mater Chem 13:700
118. Watanabe N, Kihara N, Furusho Y, Takata T, Araki Y, Ito O (2003) Angew Chem Int Ed 42:681

119. Dürr H, Bossmann S (2001) Acc Chem Res 34:905 (and references therein)
120. Klumpp T, Linsenmann M, Larson SL, Limoges BR, Bürssner D, Krissinel EB, Elliott CM, Steiner UE (1999) J Am Chem Soc 121:1076
121. Imahori H, Sakata Y (1999) Eur J Org Chem 64:2445 (and references therein)
122. Borgström B, Johansson O, Lomoth R, Berglund Baudin H, Wallin S, Sun L, Åkermark B, Hammarström L (2003) Inorg Chem 42:5173
123. Polson M, Fracasso S, Bertolasi V, Ravaglia M, Scandola F (2004) Inorg Chem 43:1950 (Punit)
124. Armaroli N (2001) Chem Soc Rev 30:113 (Punit)
125. Li K, Schuster DI, Guldi DM, Herranz MA, Echegoyen L (2004) J Am Chem Soc 126:3388–3389 (D/A units)
126. Weiss EA, Chernick ET, Wasielewski MR (2004) J Am Chem Soc 126:2326
127. Holten D, Bocian DF, Lindsey JS (2002) Acc Chem Res 35:57
128. Guldi DM (2002) Coord Chem Rev 31:22
129. Barigelletti F, Flamigni L (2000) Chem Soc Rev 29:1
130. Lainé P, Amouyal E (1999) Chem Commun Cambridge(10):935
131. Lainé P, Bedioui F, Ochsenbein P, Marvaud V, Bonin M, Amouyal E (2002) J Am Chem Soc 124:1364
132. Lainé P, Bedioui F, Amouyal E, Albin V, Berruyer-Penaud F (2002) Chem Eur J 8:3162
133. Hu YZ, Tsukiji S, Shinkai S, Oishi S, Hamachi I (2000) J Am Chem Soc 122:241
134. Johansson O, Borgström M, Lomoth R, Palmblad M, Bergquist J, Hammarström L, Sun L, Åkermark B (2003) Inorg Chem 42:2908
135. Ciofini I, Lainé P, Bedioui F, Adamo C (2004) J Am Chem Soc 126:10763
136. Adamo C, Barone V (1999) J Chem Phys 110:6158
137. Zhou X, Ren AM, Feng JK (2005) J Organomet Chem 690:338
138. Gaines GL, O'Neil MP, Svec WA, Niemczyk MP, Wasielewski MR (1991) 113:719
139. Teki Y, Miyamoto S, Iimura K, Nakatsuji M, Miura Y (2000) J Am Chem Soc 122:984
140. Teki Y, Nakatsuji M, Miura Y (2002) Mol Phys 100:1385
141. Roques N, Gerbier P, Nakajima S, Teki Y, Guérin C (2004) J Phys Chem Sol 65:759
142. Teki Y, Kimura M, Narimatsu S, Ohara K, Mukai K (2004) Bull Chem Soc Jap 77:95
143. Teki Y, Nakajima S (2004) Chem Lett 33:1500
144. Gaussian 03, Frisch MJ et al. Gaussian Inc. Wallingford CT, 2004
145. Perdew JP, Burke K, Ernzerhof M (1996) Phys Rev Lett 77:3865
146. Adamo C, Barone V (1997) Chem Phys Lett 274:242
147. Dunning TH Jr, Hay PJ (1976) In: Schaefer III HF (ed) Modern theoretical chemistry, Plenum, New York p 1
148. Hay J, Wadt WR (1985) J Chem Phys 82:299
149. Ciofini I, Daul C, Adamo C (2003) J Phys Chem A 107:11182
150. Albano G, Belser P, Daul CA (2001) Inorg Chem 40:1408
151. Fantacci S, De Angelis F, Selloni A (2003) J Am Chem Soc 125:4381
152. Hay PJ (2002) J Phys Chem A 106:1634
153. Guillemoles JF, Barone V, Joubert L, Adamo C (2002) J Phys Chem A 106:11354
154. Monat J, Rodriguez JH, McCusker JK (2002) J Phys Chem A 106:7399
155. Fantacci S, De Angelis F, Sgamellotti A, Re N (2004) Chem Phys Lett 396:43
156. Zheng KC, Wang JP, Peng WL, Shen Y, Yun FC (2002) Inorg Chim Acta 328:247
157. Zheng KC, Shen Y, Wang JP, Liu XW, Yun FC (2002) Inorg Chim Acta 335C:100
158. Xie ZZ, Fang WH (2005) J Mol Struct Theochem 717:179
159. Craig, DC, Scudder ML, McHale WA, Goodwin HA (1998) Aust J Chem 51:1131
160. Maestri M, Armaroli N, Balzani V, Constable EC, Cargill Thompson AMW (1995) Inorg Chem 34:2759
161. McCusker JK (2003) Acc Chem Res 36:876
162. Lainé PP, Ciofini I, Ochsenbein P, Amouyal E, Adamo C, Bedioui F (2005) Chem Eur J 11:3711
163. Luisi PL (2002) Foundations of Chemistry 4:183